Revista Brasileira de Física, Vol. 3, N.° 2, 1973

Effective Magnetic Dipole Operators and the Lifetime of the $3/2^-$ State in ^{207}Pb

M. DOST* and J. D. ROGERS

Rutgers, The State University, New Brunswick, NJ 08903 *and*
Instituto de Física, Universidade Federal do Rio Grande do Sul'', Porto Alegre RS

Recebido em 13 de Janeiro de 1973

A lifetime of $\tau = (0.15 \pm 0.03)$ psec for the 897 keV $3/2^-$ state in ^{207}Pb is determined by the Doppler shift attenuation method in thick Target Coulomb excitation by 68 and 61 MeV ^{16}O ions on ^{207}Pb. The analysis uses the Monte Carlo method to treat the slowing down of the recoiling Pb nuclei in Pb, and takes into account the effects of particle-γ angular correlations, finite detector size, and the slowing down of the projectiles in the target. The derived value of $B(M1, 3/2^- \rightarrow 1/2^-) = (0.52 \pm 0.10)\left(\frac{eh}{2mc}\right)^2$ can not be described with the same effectiva magnetic moment operator as describes the magnetic dipole moments in nuclei around ^{208}Pb.

A vida média de $\tau = (0.15 \pm 0.03)$ ps do nível $3/2^-$ a 897 keV no ^{207}Pb foi determinada pelo método de atenuação do deslocamento de Doppler em alvo grosso de ^{207}Pb, usando excitação Coulombiana por ions de ^{16}O de 68 e 61 MeV. Na análise utiliza-se o método de Monte Carlo para tratar o freamento dos nucleos de Pb recuando em Pb, levando em conta os efeitos de correlacões angulares partícula-y, tamanho finito do detector e freamento dos projéteis no alvo. O valor obtido de $B(M1, 3/2^- \rightarrow 1/2^-) = (0.52 \pm 0.10)\left(\frac{eh}{2mc}\right)^2$ não pode ser descrito com o mesmo operador efetivo de momento magnético que descreve os momentos magnéticos dipolares em núcleos vizinhos do ^{208}Pb.

Introduction

The magnetic moments of odd-A nuclei are known to show large systematic deviations from the Schmidt values, especially for heavier nuclei'. Determination of the magnetic properties of states consisting of a single particle

---

'Work partially supported by the National Science Foundation (USA), *Banco Nacional de Desenvolvimento Econômico* (BNDE) and *Conselho Nacional de Pesquisas* (CNPq).
*Present address: *Institut für Kernphysik der Universitat, Universitatstrasse* 14, *5-Koln-41,* Germany.
Postal address: Avenida Luiz Englert s/n, 90000 - Parto Alegre RS.

or single hole outside of a double closed shell are especially important in understanding the sources of this deviation, since these states are presumed to have particularly simple description in terms of the shell model[2].

It is noteworthy that in the vicinity of ^{208}Pb still rather few data on the magnetic properties of the "single particle" or "single hole" states are available today[3], undoubtedly due to the difficulty[4] of direct measurements of transition rates in the very heavy nuclei. This lack of data hampers a quantitative discussion as to what extent core polarization effects are state dependent, and makes a meaningful comparison of theories of the magnetic core-polarization[3-5] with experiment essentially impossible.

In the following we report on a direct measurement of the lifetime of the $3/2^-$ state at *897* keV in Pb^{207} by the Doppler shift attenuation technique[6]. The experiment consisted in a measurement of the Doppler broadened line following Coulomb excitation with ^{16}O ions of *68* and *61* MeV, respectively. The experimental details are discussed in Section 1. The experimental line shapes were compared to lineshapes synthetized by a Monte Carlo computer program to determine the lifetime. A detailed discussion of the program, and the results are given in Section 2. The program written for this purpose describes the slowing down of Pb in Pb by the Lindhard, Scharff, Schiøtt (LSS) theory evaluated by a Monte Carlo technique that treats multiple nuclear scattering exactly, calculates thick target Coulomb excitation, the influence of the particle-γ angular correlation and of the efficiency profile of the finite γ-detector on the extraction of the lifetime from the Doppler shifted spectrum. Finally, in Section 4, we compare our results to the lifetime value previously derived from the $E2/M1$ mixing ratio by Klapdor *et al.*[20] and to results of DSAM measurements carried out at other laboratories simultaneously with this measurement. The theoretical implications of the result are also discussed.

1. Experimental Details

Nuclei of ^{207}Pb in a thick target of an isotopically enriched thick target were Coulomb excited by ^{16}O ions of 68 MeV and 61 MeV produced by the Bell-Rutgers tandem Van de Graaff accelerator. The target thickness was sufficient to stop the ^{16}O beam. The beam current used was in the average *100* nA (7+) on target. The resulting singles spectra were detected by a coaxial Ge(Li) detector of 40 cm^3 with a resolution of 2.8 keV at 835 keV (Mn^{54} source)[7] placed at 3.8 cm to *17* cm from the target, depending on angle. The spectra were stored in a 4096 channel analyzer using

servo stabilization. Spectra of ^{54}Mn and ^{137}Cs were accumulated simultaneously with the experimental spectra to monitor against possibilities of gain shifts in the equipment and check calibration.

Spectra were taken with the detector at 0°, 45°, 90" and 130° with respect to the beam axis at 68 MeV, and at 0°, 45" and 90" at 61 MeV. The maximum energy of 68 MeV was chosen according to the prescription of Ref. 8 for "safe energies" to ensure that pure Coulomb excitation was involved, and in order to minimize cascade feeding from the excitation of higher levels. The energy of 61 MeV is the "safe energy" according to Ref. 9. This is important since it is necessary to know the angular distribution of the recoil nuclei and the particle-gamma angular correlation accurately in interpretation of the experimental lineshapes in singles spectra.

At the smallest distance between detector and target, the detector crystal subtends an angle of 44° at the beam spot. It is then no longer justified to calculate the Doppler shift as if the y-rays were emitted towards a point counter. We therefore measured, for each distance involved in the experiment, the efficiency as function of the angle of incidence on the Ge(Li) detector. For this we used, in a separate series of measurements, a collimated Mn^{54} source of 835 keV. The efficiency profile thus obtained is shown, for two distances of detectors, in Fig. 1.

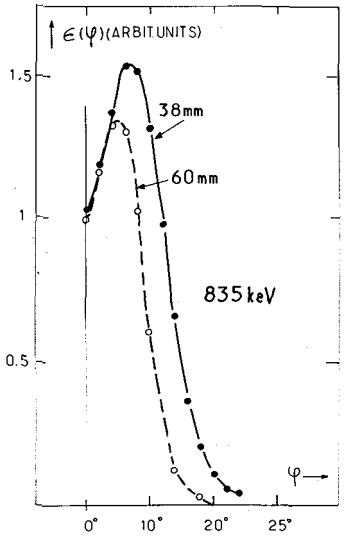

Fig. 1 - Ge(Li) photopeak efficiency ε as function of angle of incidence ϕ, for two distances between collimated ^{54}Mn (835 keV) source and the Al cap of the detector. The angle where $\varepsilon(\phi)$ becomes zero corresponds to the geometrical edge of the Ge crystal.

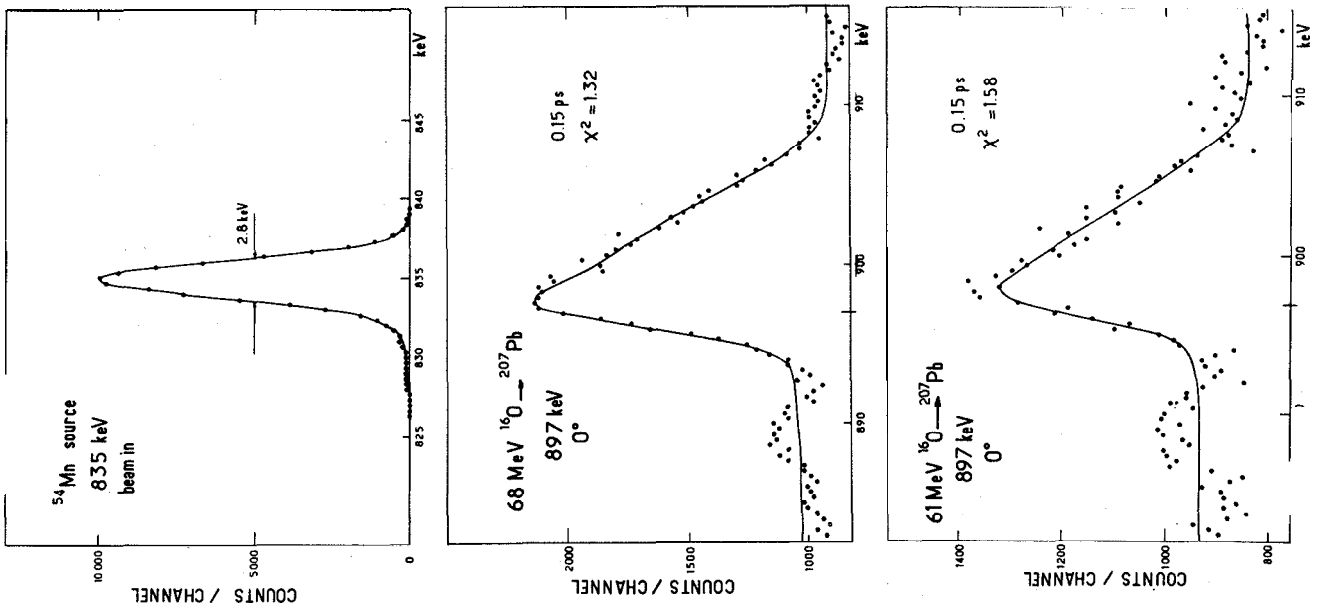

Fig. 2 - Gamma-ray single spectra at 0° with respect to the beam axis. Top: 835 keV line of the ^{54}Mn radioactive source measured with beam on target, simultaneously with the 897 keV transition in ^{207}Pb. This line is used as reference shape for the detector resolution. *Center and bottom:* Shape of the 897 keV gamma-ray peak after Coulomb excitation by 68 MeV and 61 MeV ^{16}O, respectively. The solid curve represents the theoretical lineshape calculated for $\tau = 0.15$ ps. The normalized χ^2 is also given.

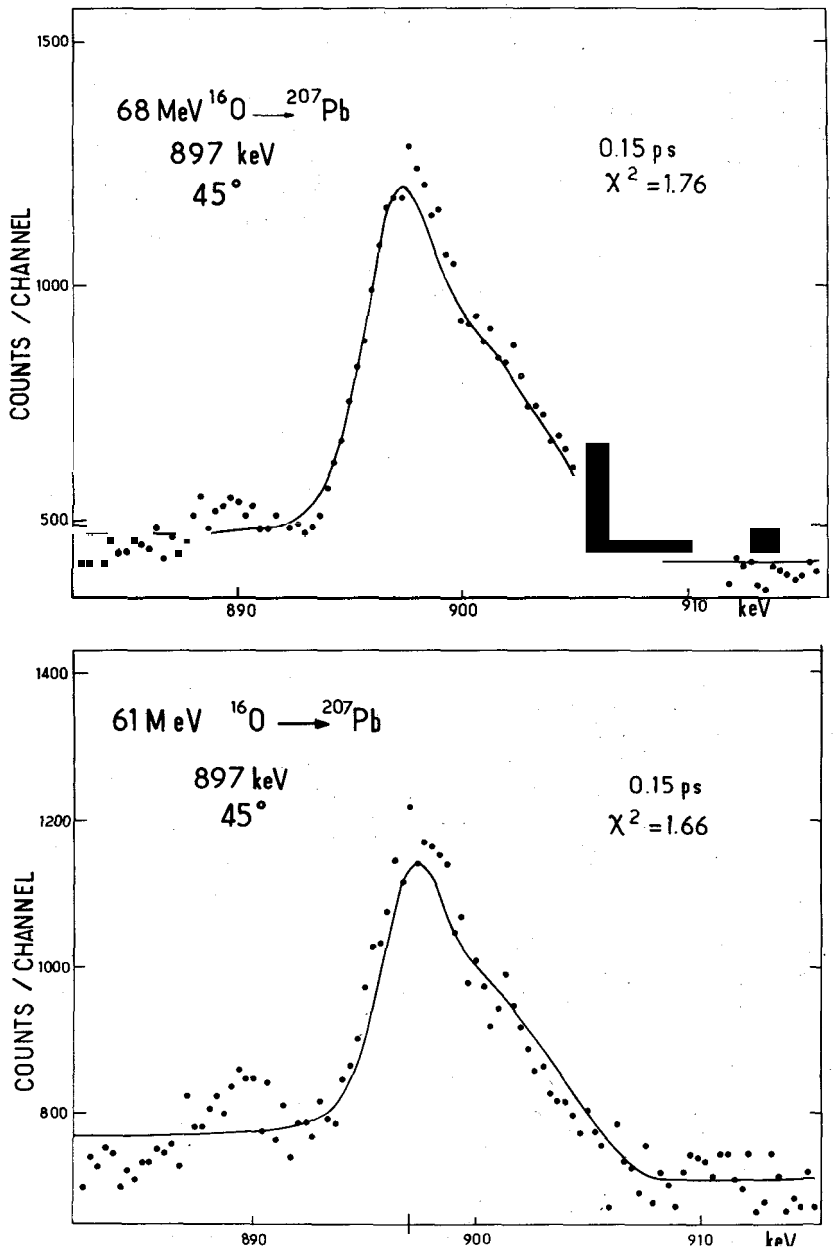

Fig. 3 - Same as Fig. 1 (center and bottom) for detector at 45°

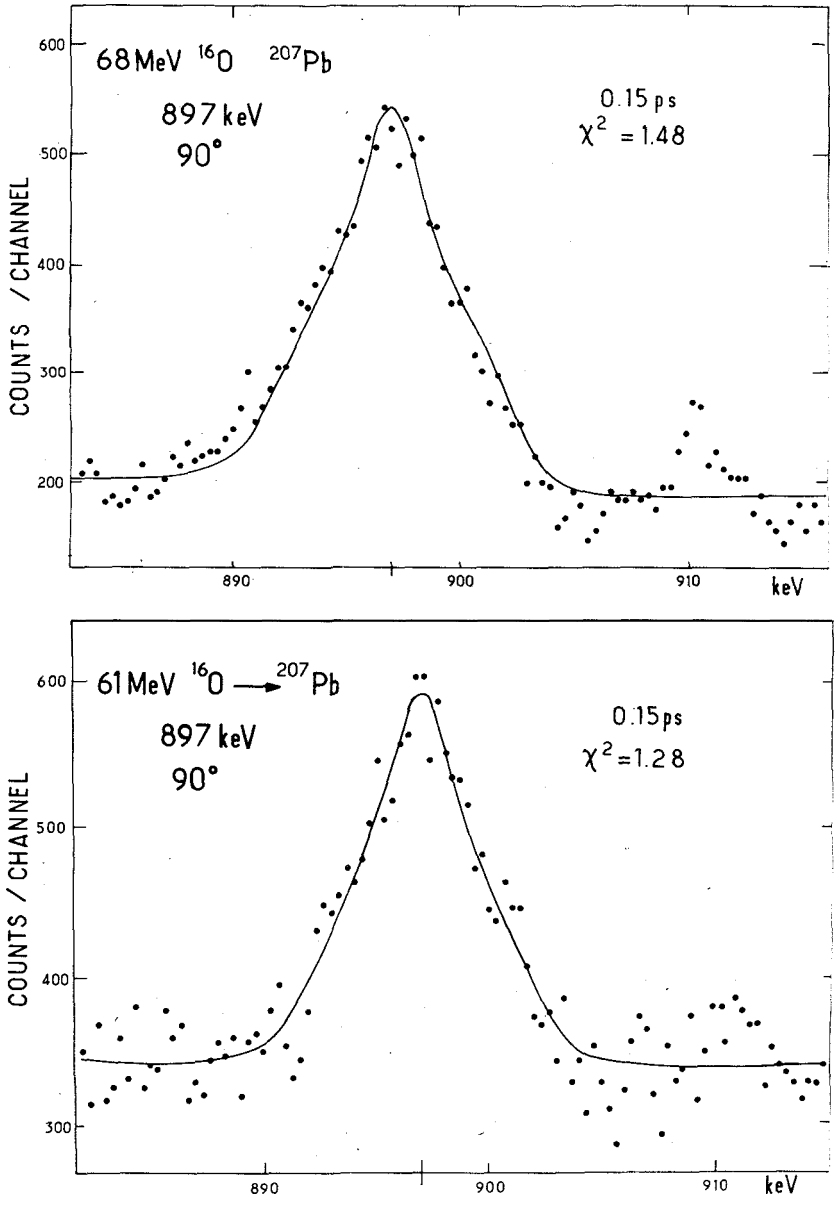

Fig. 4 - Same as Fig. 1 (center and bottom) for detector at 90°. In the spectrum at 61 MeV bombarding energy, the weak background line at 890 keV, visible in Fig. 1, has been subtracted from the data.

The final spectra obtained represént the result of about 4 days of effective machine time with an average intensity of 100 nA on target. In Figs. 2 to 5 the data are presented. There have been no corrections made to the data, except for the cases of the 90" spectrum at 61 MeV (Fig. 4, bottom half) and the 130" spectrum at 68 MeV (Fig. 5) where a small contribution from a background line at 890 keV has been subtracted out before the line shape fitting since it overlapped the Doppler broadened line.

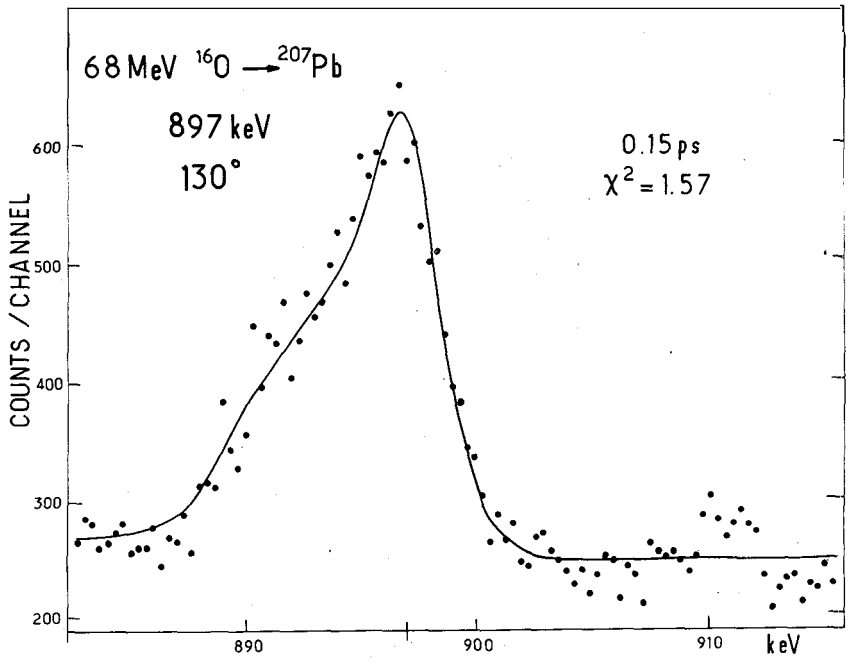

Fig. 5 - Same as Fig. 1 (center) for detector at 130". The weak background line at 890 keV, visible in Fig. 1, has been subtracted from the data.

2. Interpretation of the Observed Line Shapes

If Doppler broadened y-ray lineshapes result from thick target Coulomb excitation and are not detected in coincidence with the inelastically scattered particles, they show little structure, due to the integration over the recoil angular distributions for all projectile energies, from the beam energy down to zero. The characteristic features to be interpreted in terms of a lifetime of the decaying state are then essentially the width and displace-

ment of the roughly (in general asymmetric) triangular shaped line. It is clear that the difficulties inherent already in the interpretation of lines detected in coincidence with the inelastic particles[10,11] are accentuated in such a situation, where the interpretation depends on small details. Among the number of difficulties, we mention the following:

i) The initial Coulomb excitation takes place with a distribution of energies from the beam energy down to zero. Connected with this there is a simultaneous change of direction of the ^{16}O projectiles. Thus, in principle, the initial Coulomb excitation takes place with a distribution of projectile energies and directions.

(ii) The angular distribution of the recoil particles after E2 Coulomb excitation[12] is quite broad and has its maximum at a fairly large angle with respect to the beam direction ($\approx 80°_{lab}$ for 68 MeV ^{16}O; $\approx 60°_{lab}$ for 40 MeV ^{16}O). It also changes its shape with projectile energy, in a way which can in practice only be calculated for pure Coulomb excitation.

(iii) Since, in the excitation of heavy nuclei, the recoil energies produced are comparatively small, the relative importance of nuclear to electronic slowing down increases[10,11,13], and with it the effects of large angle nuclear scattering and associated large elastic energy loss. These effects thus become more difficult to treat in an average fashion[10,11]. This is especially important for lifetimes (τ) that allow multiple scattering of the recoiling ion in the interval of one or a few τ. This means that an accurate treatment of the time behaviour of the recoil ***direction*** has to be attempted. It has been remarked by Blaugrund several years ago that the angular effects of nuclear scattering on the Doppler shifted spectrum can be larger than the effects due to changes of kinetic energy of the recoiling ions alone[13]. For the evaluation of these effects only an individual collision-by-collision treatment is at hand. Moreover, as the nuclear stopping becomes comparable to the electronic stopping, the ratio of the two becomes a more sensitive parameter[14].

(iv) As the y-ray lines from thick target Coulomb excitation are intrinsically rather structureless, it is worth considering the influence of the effect of the large angle subtended by the Ge(Li) detector on the distribution of Doppler shifts. The influence of the particle-y angular correlation function becomes stronger and so does the effect of the efficiency profile of the finite detector at the given energy. It is evident that for the same reason (small excitation cross section) that one uses the the thick target, one also uses the Ge(Li) detector at small distances from the target. So these additional effects tend to arise together.

Due to the above mentioned difficulties, it was not felt adequate to attempt to interpret the observed lineshapes by means of using the usual approximations of an effective thick target energy[12] for the Coulomb excitation and using the approximation of Blaugrund[13] for the effects of nuclear scattering. It was therefore decided to use the Monte Carlo technique to generate simulated line-shapes. To our knowledge, there exists so far for the heaviest nuclei no treatment of Doppler line shapes from thick target excitation using the Monte Carlo technique that also includes the effects of finite detector and particle-y correlation. The recently published Monte Carlo program of Currie[10] neglects these latter effects, while the program of Stokstad *et al.*[14] includes them, but uses the Blaugrund approximation for the angular effects of nuclear scattering. We found it therefore worthwhile to write such a program[15]. An effort was made to take into account all possible presently understood effects that could significantly affect the lineshape. We have however assumed that the spin of the recoiling nucleus undergoes no deorientation in collisions. We have also neglected changes of direction of the projectile while it slows down.

The program is based on a Monte Carlo evaluation of the Lindhard, Scharff, Schiøtt (LSS) theory[16] for the slowing down of the recoil ions. Most of the basic formulas on which this part of the program is based were given by Currie[10]. The program produces a series of ion histories and samples the velocity and direction at the time of each y-emission.

The program used has three major sections. The first consists of the construction of a 2000 place table of angle and energy starting values for the recoil ions. The second treats the slowing down of the recoils, by evaluating the LSS slowing down theory, collision by collision by a Monte Carlo technique[10]. The third major section uses the information on ion velocity and direction at the y-emission time, obtained in the second section, to produce the Doppler shifted y-ray spectrum. In this section, effects of particle-γ angular correlation and the geometry and efficiency of the finite γ-detector are also taken into account.

The principal steps in computing are the following:

(i) table of starting values in the case of Coulomb excitation:

The energy between the ^{16}O bombarding energy and the ^{16}O energy at which the angle integrated Coulomb excitation yield has dropped to 3% of the initial value, is divided into 20 intervals such that each of them carries 1/20 of the energy and angle integrated Coulomb excitation yield. Values

of the ^{16}O energy loss in Pb are taken from Booth and Grant[17]. The interval of ^{16}O inelastic scattering angles is covered with a 100 interval grid, each of the intervals representing 1/100 of the angle integrated excitation cross section at the particular ^{16}O energy in question. The equations of Alder *et al.*[12] were used. Thus, the angle as well as energy intervals are not equidistant. By choosing angles and energies randomly from this table, proper care is taken of the weightings with the energy and angle dependent Coulomb excitation probability in order to start the recoil ion histories with the correct probability distribution of directions and velocities. The table had to be prepared only once for each ^{16}O bombarding energy. The subroutine CURK, written by G. Seaman[18], was incorporated in the program to calculate the orbital integrals involved.

(ii) Monte Carlo treatment of slowing down:

The theory of LSS[16] gives the stopping power as

$$\frac{d\varepsilon}{d\rho} = \left(\frac{d\varepsilon}{d\rho}\right)_{electronic} + \left(\frac{d\varepsilon}{d\rho}\right)_{nuclear} = k_e \varepsilon^{1/2} + \frac{1}{\varepsilon} \int_0^{\varepsilon} f(x)\,dx,$$

with generalized dimensionless "energy" ε and "distance" ρ and the electronic slowing down constant k_e defined in Refs. 10, 16. The function $f(x)$ generates the cross section σ_n of the nuclear collisions for a screened Coulomb potential according to $\sigma_n(\varepsilon) = \pi a^2 \int_0^{\varepsilon} x^{-2} f(x)\,dx$ with a being the Bohr radius. The function $f(x)$ is also given in Refs. 10, 16. We used it with the numerical constants given by Currie[10] for a Thomas-Fermi atom.

The recoil energy and direction were chosen randomly from the table of starting values constructed in the first section. Given the value of the coefficient $A_2^{(2)} = -0.163$, derived from the known[20] $\delta(E2/M1)$, these two values determine already the particle-y angular correlation functiou (**Eq.** II A.66 of Ref. 12) for the y-ray emitted later in the history of the recoiling nucleus. Thus, the value of this angular correlation function was calculated for each of 45 segments on the detector surface, to be used as a weighting factor. Also, a table of up to 20 independent emission times was set up, corresponding to the expression

$$t_k^{\text{emission}} = \tau \log\left(\frac{1}{1-P_k}\right), \quad k = 1, 2, \ldots 20,$$

for the chosen lifetime τ. Here, P_k is a random number between 0 and I, representing the probability at time t, for the excited nucleus to have already emitted its y-ray. One recoil ion track can in this way be used to produce, in the calculation, more than one count in the γ-detector. It is clear that the average number of nuclear collisions limits the number of independent y-rays one can thus produce from one ion track.

The choice of energy of each succeeding nuclear collision and of scattering angle and associated elastic energy loss were done in a way very similar to that described by Currie[10], with the modification that the nuclear scattering cross section was represented as a function of energy instead of distance (this means neglect of ion range compared to detector distance.) The time between two subsequent nuclear collisions is determined by the exponentially decreasing velocity, due to electronic stopping given by the constant k_e (or the equivalent electronic slowing down time a). Thus the electronic energy loss $E, -\varepsilon_0$ between nuclear collisions translates into the time scale t via the relationship $At = (1/2)\alpha \log(\varepsilon_0/\varepsilon_1)$. When t passes the next y-ray emission time t_k^{emission} for that ion track, the program goes to its third major section, the actual synthesis of

(iii) the spectrum.

There, the Doppler shift for each of the segments on the detector surface is calculated from the velocity and direction of the recoil at the time of y-emission. The spectrum is incremented in the channel corresponding to each of these shifts by a fraction of a count, which is in addition weighted with the value of the angular correlation function, the solid angle, and the detector efficiency for the corresponding surface segment of the detector. Then, the next y-ray emission is treated.

After a preset number of ion tracks the process stops. The experimental detector resolution is then folded into the Doppler shifted spectrum before comparing it to the data. For a given lifetime τ, the only parameter in the χ^2 fitting is the overall normalization of this final theoretical y-ray spectrum.

Typically, 1000 tracks and 20000 counts were accumulated for each spectrum. This number of counts were produced in about 60 sec on an IBM 360 – 91. The computing time is roughly proportional to the number of tracks treated, since the slowing down section consumes the largest part of the computing time. Tests show that for a number of tracks

inferior to 1000 statistical variations of the calculated curves are not completely negligible, but they are above 1000 tracks, as is borne out by Fig. 6.

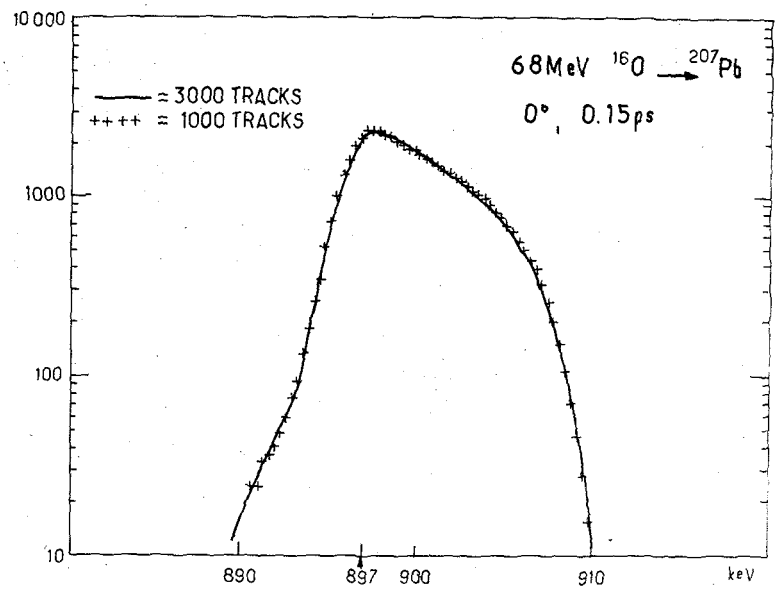

Fig. 6 - Influence of the "statistics" of the Monte Carlo calculation. A lineshape calculated from 1000 recoil ion histories is compared to one calculated from 3000.

A series of tests were made to assure the proper functioning of the program. They include the reproduction of the full Doppler shift for the detector placed at 0°, a particle detector at 180" and a lifetime $\tau \ll$ a. For the γ-detector at 90°, symmetric lines are calculated.

The Coulomb excitation part was checked by comparing angular distributions of the scattered ions as calculated from the program with the formulas given by Alder et *al.*[12]. Fig. 7 shows for one energy, that the two curves are in very satisfactory agreement. A further check of the correct handling of the Coulomb excitation comes from the fact that the effective thick target energy calculated from our table is equal to that given by Alder et *al.*[12]. Thus energy as well as angle dependence of the Coulomb excitation yield are adequately represented by the variable distance grid used as input table to the Monte Carlo simulation of the slowing down of the recoiling Pb ions.

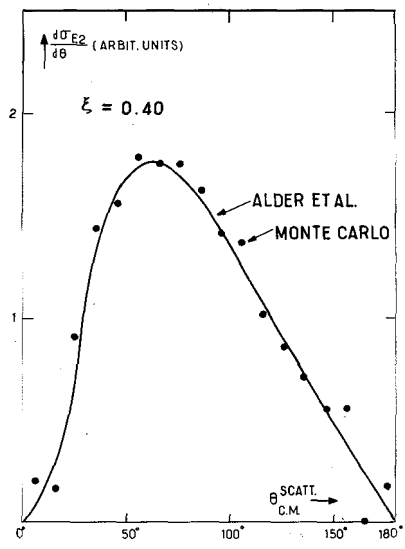

Fig. 7 - Angular distribution of the ^{16}O ions inelastically scattered in E2 Coulomb excitation at 63.5 MeV ($\xi = 0.40$) of the 897 keV $3/2^-$ state of ^{207}Pb. The solid curve is calculated directly from the formulae of Alder *et al*[12]; the points represent the distribution as reconstrucied by the Monte Carlo program from the angle table.

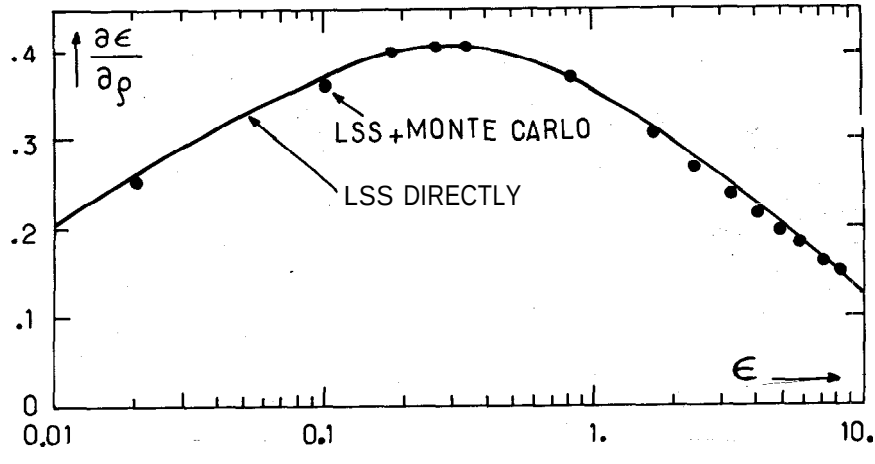

Fig. 8 - Nuclear stopping power $(d\varepsilon/d\rho)_n$ as a function of generalized energy ε of the LSS theory. The solid curve is calculated directly from this theory, the points give the values as sampled by the Monte Carlo program from the treatment of Pb-Pb collisions, using the LSS theory with the same parameters.

The slowing down part of the program was checked by comparing the energy loss of the recoil ion as a function of energy as calculated by the Monte Carlo procedure with that calculated directly from the formulas of Lindhard, Scharff and Schiøtt[16]. Fig. 8 shows the comparison for the nuclear $(d\varepsilon/d\rho)$. There is complete agreement, which proves that we evaluate the LSS theory correctly. This makes for increased confidence in the treatment of the large angle nuclear scattering. This latter can reach a substantial probability, as noticed by Currie *et al.*[11]. Comparisons between the Monte Carlo results and the approximation of Blaugrund[13] for the angular deviation due to nuclear scattering were therefore made. We find that there are systematically increasing deviations of $\langle \cos\theta \rangle$ with decreasing energy of the ion. At $\varepsilon = 0.3$, for example, $\langle \cos\theta \rangle$ obtained from the Blaugrund formulas is still 0.4 while from the Monte Carlo calculation one finds 0.33. At $\varepsilon = 0.1$, these two numbers are 0.24 and 0.15 respectively, but may contain larger numerical uncertainties. To illustrate that already at higher recoil energies deviations are present, we show in Fig. 9 the Doppler line shape with ^{16}O inelastic particles detected at 180°, and the γ-detector placed at 0°. The recoil ions start out with $\varepsilon = 2.0$. At this energy, nuclear and electronic stopping power are just equal. It is clearly visible that for such energies the Monte Carlo treatment of the LSS theory gives a markedly sharper separation of the "slow" from the "fast" component of the line than does the Blaugrund procedure. This can be understood as originating in the large angle nuclear scattering and corresponding large energy loss in single collisions neglected by Blaugrund's averaging method. Here, we agree with the conclusions of Currie et *al.*[11] who studied the slowing down of Si ions in Au and found already 20% of the ions scattered through more than 90°. Finally, we have also compared the ratio $(d\varepsilon/d\rho)_{nuclear}/(d\varepsilon/d\rho)_{electronic}$ as calculated by the program to that directly derived from the LSS curves. There is complete agreement. We therefore conclude that our Monte Carlo evaluation duplicates the LSS theory correctly, and that the smaller angular deviations for low recoil energies obtained from Blaugrund's formulas are a result of the approximations that Blaugrund's treatment makes to the LSS theory.

3. Results

A linear background was assumed to be present in the data, given by the straight line connecting the average constant background on the left and on the right of the Doppler shifted peak. Zero shift

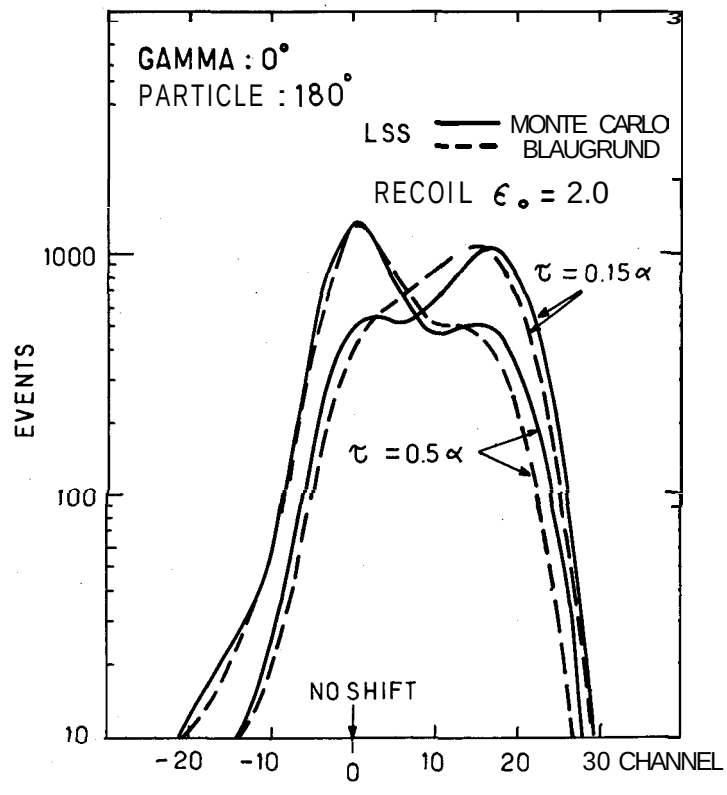

Fig. 9 - Calculated Doppler shifted lineshape: for the $3/2^- \rightarrow 1/2^-$ transition in ^{207}Pb at 0°, in coincidence with backscattered inelastic ^{16}O ions. The initial recoil energy is taken to be $\epsilon_0 = 2.0$, the value where nuclear and electronic stopping power are just equal. The recoils are slowing down to zero energy. Lifetimes are given in units of the electronic slowing down time $\alpha = 1.235 \times 10^{-12}$ sec. The curves calculated with Blaugrund's formulae show less separation between the "fast" and "slow" component of the line and would lead to the extraction of different lifetimes from the data.

calibration was done by using the position of the 90" line together with the position of the ^{137}Cs (662 keV) and ^{54}Mn (835 keV) lines which were used in all the runs to monitor electronic instabilities.

The results of the χ^2-fit to the data taken at 0°, 45°, 90" and 130" at 68 MeV bombarding energy, and at 0°, 45° and 90" at 61 MeV bombarding energy are shown on Figs. 2 to 5. Figure 2 also shows the 835 keV ^{54}Mn line used as reference for the detector resolution.

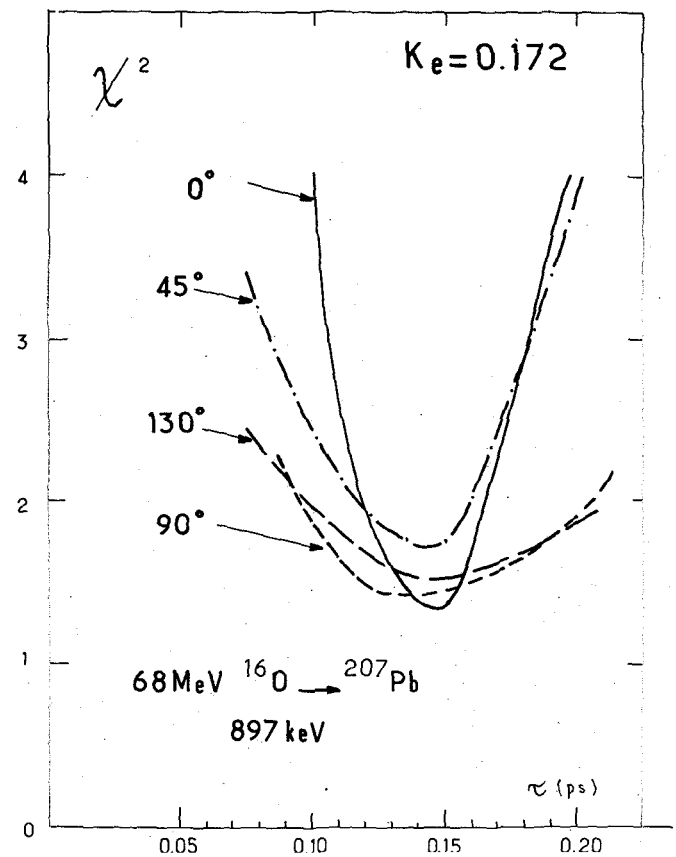

Fig. 10 - The normalized χ^2 as a function of lifetime τ that was used to calculate the theoretical lineshape, for the spectra taken at 68 MeV beam energy. The constant $k_e = 0.172$ is used in the expression for the electronic stopping power $(d\varepsilon/d\rho)_e = k_e \varepsilon^{1/2}$ of Pb recoiling into Pb.

Figures, 10 and 11 represent the χ^2 as function of the chosen lifetime τ. Of seven χ^2 curves, six give a lifetime close to 0.15 psec. The curve for 45° would give a longer lifetime, however the fit with $\tau = 0.15$ psec is still acceptable statistically, as can be seen from Fig. 3. The χ^2 curve for the spectrum at 68 MeV and 0° is the steepest of all, and we derive the error of the lifetime from the width of this curve at 1.5 times the minimum value. This gives

$$\tau = (0.15 \pm 0.03) \text{ psec}$$

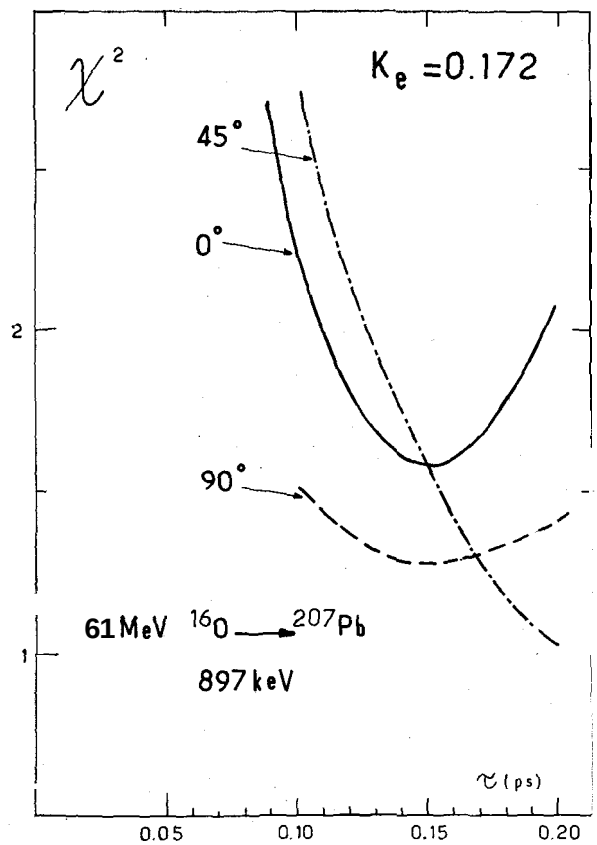

Fig. 11 - Same as Fig. 10, for the spectra taken at 61 MeV beam energy

for the lifetime of the 897 keV, $3/2^-$ state in ^{207}Pb with the error being approximately a normal one[19]. The principal source of this error is statistics in the data. It is mainly because of bad statistics and the increased influence of weak background lines that some of the χ^2 curves are much flatter than the others. Measurement at different angles and bombarding energies constitutes, however, an important test of the consistency in the data interpretation.

The quoted error does ***not*** include a systematic contribution from the insufficiently known slowing down parameters of the LSS theory[6, 11, 13, 14] An uncertainty of 20% is in general associated with the electronic stop-

ping[6,13,14]. To obtain an idea of the influence of such uncertainties of the theory, the sensitivity of our result to the ratio of electronic to nuclear stopping (as for instance specified by the constant k_e of the LSS theory) was checked. The results are shown for 0°, 68 MeV bombarding energy in Fig. 12. As was expected, the results are only moderately sensitive to this number, since the nuclear stopping is predominant for a large fraction of the recoil energies of interest. The standard value for Pb in Pb of $k_e = = 0.172$ was therefore kept in the final analysis. For the k_e of 20% higher claimed in Refs. 13, 14 the lifetime would become $\tau = (0.14 \pm 0.03)$ psec. At the same time, since the electronic stopping time a = 1.235 psec is considerably longer than the lifetime, the result obtained is not strongly dependent on the details of the stopping at very low ion velocities. We thus expect that for this case the major errors inherent in the approximations of the Lindhard-Scharff-Schiøtt theory itself, and in the numerical uncertainties of its parameters are inferior to the statistical error given above.

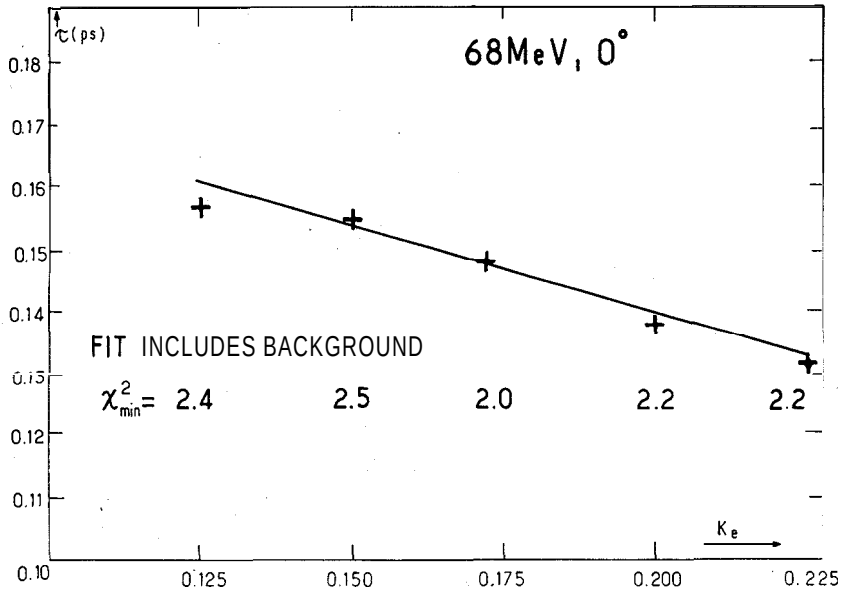

Fig. 12 - Variation of the lifetime extracted from the 68 MeV, 0° lineshape, with electronic stopping constant k,. The straight line drawn through the points is not a fit. For each point $\tau = \tau(k_e)$ the minimum χ^2 of the lineshape fit is given. It is calculated with the background on both sides of the Doppler shifted line included, in contrast to Figs. 1 to 4.

4. Discussion

Klapdor *et al.*[20] have previously used the value of the $E2/M1$ mixing ratio, 6, determined from a measurement of the angular distribution of the 897 keV gamma-ray, following Coulomb excitation of ^{207}Pb with 14.4 MeV a-particles, together with the independently known value of $B(E2) = (62 \pm 3)e^2\,fm^4$ from Grosse *et al.*[21] to deduce a value of $\tau = (0.21 \pm 0.04)$ psec for the lifetime of the $3/2^-$ state. Within the quoted errors, this result is not in disagreement with our directly determined value of $\tau = (0.15 \pm 0.03)$ psec. In work of Refs. 21 and 28 done simultaneously to that reported here values of $\tau = (0.17 \pm 0.05)$ psec and $\tau = (0.19 \pm 0.04)$ psec respectively were derived from DSAM using 80 MeV oxygen ions. In both cases the Blaugrund approximation was used to treat nuclear scattering.

Using the measured value of $\tau = (0.15 \pm 0.03)$ psec and the value of $\delta = 0.096 \pm 0.011$ for the 897 keV transition[20], we obtain for the reduced transition probability

$$B(M1, 3/2^- \to 1/2^-) = \frac{1}{\tau}\,\frac{1}{(1+\delta^2)}\cdot\frac{1}{1.76\times 10^{13}\,[E_\gamma(\mathrm{keV})]^3}\left(\frac{e\hbar}{2mc}\right)^2$$

$$= (0.52 \pm 0.10)\left(\frac{e\hbar}{2mc}\right)^2.$$

This value can be compared to the Schmidt prediction for a $p_{3/2}^{-1} \to p_{1/2}^{-1}$ neutron hole transition of

$$B_{S.P.}(M1, p_{3/2} \to p_{1/2}) = 1.16\left(\frac{e\hbar}{2mc}\right)^2.$$

The deviation observed is comparable to that found for the majority of magnetic moments in the Pb region. These discrepancies have been qualitatively explained in terms of spin polarization induced in the core by the odd particle or hole[5]. It has been shown that to first order these spin polarization effects can be expressed in terms of an effective magnetic dipole operator of the form[1,22]

$$(M1) = \left(\frac{3}{4\pi}\right)^{1/2}(\mu_{S.P.} + \delta\mu)\left(\frac{e\hbar}{2mc}\right) \qquad (1)$$

where the free nucleon moment is given by

$$\mu_{sp} = g_s \mathbf{s} + g_l \mathbf{l};$$

and $$\delta\mu = \delta g_s \mathbf{s} + \delta g'_s \{Y_2 s\}_1 + \delta g_l \mathbf{l}$$

is the additional moment due to the induced polarization in the core.

A renormalization δg_l of the orbital g-factor has been included in accordance with the experimental results of Yamazaki *et al.*[23]. The conditions for the validity of this type of description have been discussed in Refs. 1, 24, 26.

Microscopic calculations have been made for some magnetic moments by Blomquist *et al.*[24] and for both magnetic moments and M1 transition probabilities by Harada and Pittel[3]. Maier et *al.*[26] have deduced values of $\delta g_s = 3.43$, $\delta g'_s = -4.55$ and $\delta g_{ln} = -0.06$, from a fit of Eq. (1) to values of 13 magnetic moments in the region of ^{208}Pb. In order to compare their phenomenological results to the theoretical calculations we have used the same effective moment operator to parametrize the results of Harada and Pittel. Fitting Eq. 1 to their predicted $1/2^-$ and $3/2^-$ magnetic moments using $\delta g_l = 0$ we derived values of $\delta g_s = 72$ and $\delta g'_s = -.76$. With these values one reproduces their theoretical predictions to better than 5% accuracy for the static moments and the $3/2^- \rightarrow 1/2^-$ transition probability. However, the $7/2^- \rightarrow 5/2^-$ transition probability found from the effective operator is 15% too large. The values for δg_s and $\delta g'_s$ are significantly smaller in both cases than those obtained by Maier *et al.*[26].

Quantity	Maier *et al.*[a]	Harada and Pittel[b]	Schmidt Value	Experiment
$\mu(1/2^-)$	0.63	0.62 (0.58)[f]	0.64	0.59[c]
$\mu(5/2^-)$	0.49	1.17 (1.00)[f]	1.37	0.65 ± 0.05[d]
in $\left(\frac{e\hbar}{2mc}\right)$				
$B(M1, 3/2^- \rightarrow 1/2^-)$	0.01	0.71	1.16	0.52 ± 0.10[e]
in $\left(\frac{e\hbar}{2mc}\right)^2$				

a) Ref. 26; $g_s = -3.82$, g, = 0, $\delta g_s = 3.43$, $\delta g_l = -0.06$, $\delta g'_s = -4.55$
b) Ref. 3; we quote the values for Gillet's CAL force;
c) Ref. 27; error smaller than 0.01 $\left(\frac{e\hbar}{2mc}\right)$;
d) Ref. 28;
e) this work;
f) value corrected for $\delta g_{ln} = -0.06$.

Table I - The known magnetic moments and the reduced M1 transition probability in ^{207}Pb together with the values predicted by Maier *et al.* (Ref. 26) and Harada and Pittel (Ref. 3).

In Table I, we compare the known values for magnetic dipole moments

and transition rates in ^{207}Pb to the theoretical predictions of Harada and Pittel[3] and to the values given by Maier *et al.*[26]. We conclude from this comparison that the simplified model of a state independent effective moment operator is able to explain in a qualitative way the deviations of the static and transition moments from the Schmidt values. However, no quantitative agreement is obtained. On the other hand, it is clear that the microscopic calculations also do not succeed in reproducing the experimentally determined moments and transition rates.

We would like to thank the staffs of the computing centers of the University of Rio Grande do Sul, the Department of Physics of the University of São Paulo and the *Département de Calcul Elétronique* of the C.E.N. de Saclay for assistance in development of the program used in the lineshape analysis. One of us (M.D.) also takes the opportunity to thank the *Instituto de Física* of the University of Rio Grande do Sul at Porto Alegre for two months of hospitality during which we did a large part of the programming.

References and Notes

1. E. Bodenstedt and J. D. Rogers, in *Perturbed Angular Correlations,* ed. by E. Karlsson, E. Mathias and K. Siegbahn; North Holland Publishing Co., Amsterdam (1964), pg. **21.**
2. J. D. Vergados, Phys. Lett. **34B, 121 (1971).**
3. K. Harada and S. Pittel, Nucl. Phys. **A159, 209 (1970).**
4. 0. Hausser and D. Ward, BAPS **15, 805 (1970).**
5. A. Arima and H. Horie, Progr. Theoret. Phys. (Kyoto) **12, 623 (1954).**
6. A. Z. Schwarzschild and E. K. Warburton, Ann. Rev. Nucl. Sci. **18, 265 (1968).**
7. We thank the group of N. Koller and J. W. McDonald for having lent us one of their Ge(Li) detectors for several runs at the tandem accelerator.
8. J. De Boer and J. Eichler, Advan. Nucl. Phys., Vol. 1, **1 (1968).**
9. D. Cline, H. S. Gertzman, H. E. Gove, P. M. S. Lesser, and J. J. Schwartz, Nucl. Phys. **A133, 445 (1969).**
10. W. M. Currie, Nucl. Instr. Meth. **73, 173 (1969).**
11. W. M. Currie, L. G. Earwaker, and J. Martin, Nucl. Phys. **A135, 325 (1969).**
12. K. Alder, A. Bohr, T. Huus, B. Mottelson and A. Winther, Revs. Mod. Phys. **28,432 (1956).**
13. A. E. Blaugrund, Nucl. Phys. **88, 501 (1966).**
14. R. G. Stokstad, I. A. Fraser, J. S. Greenberg, S. H. Sie, and D. A. Bromley, Nucl. Phys. **A156, 145 (1970).**
15. The FORTRAN deck of the program and the listing are available from one of us (M.D.) at *Institut für Kernphysik der Unioersitat,* 5-Koln-41, Germany.
16. J. Lindhard, M. Scharff, and H. E. Schiøtt, Mat. Fys. Medd. Dan. Vid. Selsk **33,** N.° **14 (1963);** J. Lindhard, V. Nielsen and M. Scharff, *ibid.* 36, *N.°* **10 (1968).**
17. W. Booth and I. S. Grant, Nucl. Phys. **63, 481 (1965).**
18. S. Steadman, private communication.
19. e g. N. L. Johnson and F. C. Leone, *Statistics and Experimental Design,* Wiley and Sons, Inc., New York, London, Sidney **(1964).**
20. H. V. Klapdor, P. von Brentano, E. Grosse, and K. Haberkant, Nucl. Phys. **A152,** 263 **(1970).**
21. E. Grosse *et* al., preprint *MPI* Heidelberg (1971).
22. A. Bohr and B. Mottelson, Nuclear Structure, Vol. 1, Benjamin, New York **(1969).**
23. T. Yamazaki, T. Nomura, S. Nagamiya, and T. Katou, Phys. Rev. Lett. **25, 547 (1970).**

24. J. Blomqvist, N. Freed, and H. O. Zettzerstrom, Phys. Lett. 18, 47 (1965).
25. V. Gillet, A. M. Green, and E. A. Sanderson, Nucl. Phys. 88, 321 (1966).
26. K. H. Maier, K. Nakai, J. R. Leigh, R. M. Diamond, and R. S. Stephens, preprint UCRL - 19593 (1970).
27. Table of Nuclear Moments, compiled by V. Shirley, in *Hyperfine Structure and Nuclear Radiation,* eds. E. Matthias and D. A. Shirley (North-Holland Publishing Co., Amsterdam 1968).
28. H. J. Koerner, K. Auerbach, J. Braunsfurth, and E. Gerdau, Nucl. Phys. **86,** 395 (1966).